Macromolecules

Volume 24, Number 8 April 15, 1991

Synthesis and Physical Properties of Liquid-Crystalline Polyesters Derived from 4,4′-Dihydroxybicyclohexyl

A. Coassolo, M. Foá,* D. Dainelli,† R. Scordamaglia, L. Barino, and L. L. Chapoy‡

Himont Novara, via Caduti del Lavoro, 28100 Novara, Italy

F. Rustichelli, B. Yang, and G. Torquati§

Università di Ancona, via Ranieri-Monte D'Ago, 60100 Ancona, Italy

Received May 1, 1990; Revised Manuscript Received August 29, 1990

ABSTRACT: Liquid-crystalline polyesters have been prepared from the mesogenic unit 4,4′-dihydroxybicyclohexyl and linear aliphatic diacids, which served as a flexible spacer. The polymers were characterized by optical microscopy, thermal analysis, X-ray diffractometry, and conformational analysis. The polymers have been assigned as passing through the following thermotropic transition sequences: crystal–smectic G–isotropic. This behavior is compared with that of the corresponding polymers prepared from 4,4′-dihydroxybiphenyl.

(I) Introduction

Several examples of main-chain liquid-crystalline thermotropic polyesters derived from *trans*-cyclohexanedicarboxylic acid and/or *trans*-cyclohexanediol are known from the literature.[1] Despite the large difference in steric configuration and chemical behavior, the *trans*-cyclohexyl moiety and phenyl ring seem to be very similar with respect to their rigidity, linearity, and ability to behave as a mesogenic unit. Main-chain LCP's with linear, rigid mesogenic units are known to show high glass transition and melting temperatures, in some cases even exceeding the onset of decomposition. Therefore, as in the aromatic series, the melting point of polyesters containing the *trans*-cyclohexyl group as the mesogenic unit must be decreased by modifying the rigidity and linearity of the structure through the use of nonlinear comonomers, comonomers containing lateral substituents, or flexible spacers in the main chain.[1]

The behavior of the *trans*-cyclohexyl moiety prompted us to study the possibility of obtaining main-chain thermotropic polyesters containing only the *trans,trans*-bicyclohexyl group as the mesogenic unit. We were also interested in assessing the influence of this group on liquid crystallinity in comparison with that of the biphenyl moiety. To the best of our knowledge, there are only a few examples of low molar mass liquid crystals containing the *trans,trans*-bicyclohexyl unit[2] and only one example[3] of a main-chain thermotropic polyester. However, in this latter case the mesogenic unit is the trimer sequence hydroxybenzoic acid–*trans,trans*-dioxybicyclohexyl–hydroxybenzoic acid with a polysiloxane flexible spacer.

In the present paper we report the synthesis and characterization of liquid-crystalline homopolyesters obtained by the polycondensation of *trans,trans*-4,4′-dihydroxybicyclohexyl with linear-chain dicarboxylic acid chlorides.[4]

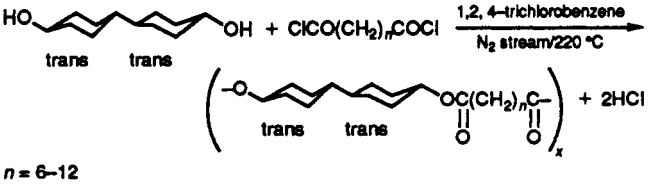

The *trans,trans*-4,4′-dihydroxybicyclohexyl was obtained by the hydrogenation of 4,4′-dihydroxybiphenyl and subsequent separation of the stereoisomers.[5]

† Current address: M&G Ricerche, via Montichio km 0.200, Ferentino (FR), Italy.
‡ Current address: Montefluos, via S. Pietro 50, 20021 Bollate (MI), Italy.
§ Deceased.

0024-9297/91/2224-1701$02.50/0

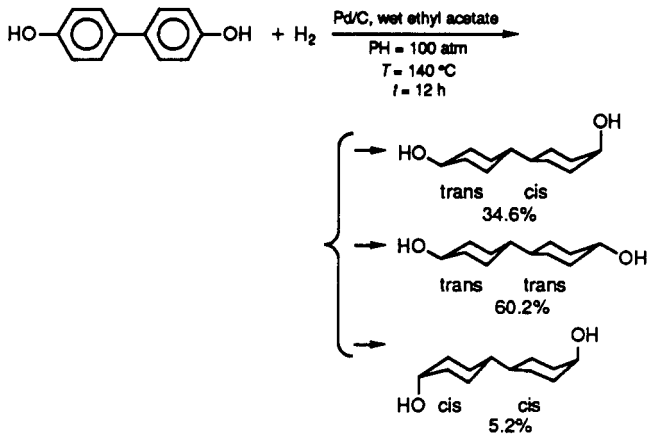

The preparation of semiflexible polymers has been chosen in order not only to modify their transition temperatures[6] but also to compare their properties with those of the corresponding polymers derived from 4,4′-dihydroxybiphenyl.[7,8]

(II) Experimental Section

The thermal behavior of the polymers was studied with a Perkin-Elmer DSC-7 calorimeter calibrated with indium and tin standards. Weighed samples (5–10 mg) of polymers were placed in an aluminum pan, heated at a fixed heating rate (5–20 °C/min) up to a clearing point, and then cooled to room temperature at a fixed rate (5–20 °C/min). In all cases the first and the second runs were recorded.

The thermal stability of the polymers was checked with a Perkin-Elmer TGA-7 thermogravimetric analyzer, operating under nitrogen. Samples (3–5 mg) were placed in an aluminum holder and heated at 20 °C/min up to 500 °C, while the percent weight loss was recorded against temperature.

Optical observations were performed by an Olympus Vanox optical microscope equipped with a Linkam THM 600 hot stage. Samples were placed between two glass slides and heated or cooled at 1–10 °C/min under a nitrogen stream in order to prevent oxidative degradation. Shearing between the slides was used as a qualitative evaluation of melt viscosity.

Inherent viscosities of the polymers were measured with an Ubbelohde viscosimeter in a thermostated bath at 30 °C. The concentration of the solutions was 0.25 g/dL in a 60/40 by weight phenol/tetrachloroethane mixture.

X-ray diffraction experiments were performed by a rotating anode generator Rigaku Denki RV 300 with a small-angle medium-resolution vacuum pin-hole camera. Clear, high-resolution scattering photographs were obtained by reducing air scattering by either evacuating the camera or filling it with helium gas. The percent crystallinity is estimated from the relative intensity of the crystalline reflections to the total scattering intensity. Nickel-filtered Cu Kα X-ray radiation was used.

Preparation of *trans,trans*-4,4′-Dihydroxybicyclohexane.[5] A 1-L autoclave was charged with 40 g of 4,4′-dihydroxybiphenyl (Schenectady Chemical Inc.), 500 mL of ethyl acetate containing 1% water, and 4 g of palladium supported on activated carbon containing 50% water (5% of metallic Pd on the dry support). After elimination of air by purging with nitrogen and hydrogen, 80 atm of hydrogen was charged. The reaction mixture was heated to 140 °C and stirred at that temperature for 12 h. After cooling to room temperature, the catalyst was recovered by filtration and the solvent was evaporated. The gas chromatographic analysis of the crude product (42.4 g) showed complete conversion of the starting reagent; 4,4′-dihydroxybicyclohexane was obtained with 99.5% selectivity, the remaining being hydrogenolysis products. The three possible stereoisomers were identified by gas–mass analysis, and the isomeric composition was established by gas chromatography (trans,trans, 60.2%; cis,trans, 34.6%; cis,cis, 5.2%). After repeated crystallization from chloroform, 18 g of the trans,trans isomer was isolated (purity ≥99%) with a melting point at 214–215 °C.[9] In Figure 1 we report its ^{1}H NMR spectrum in perdeuteriodimethyl sulfoxide. The spectrum was characterized by the presence of a doublet at 4.5 ppm (two protons of OH groups), a multiplet at 3.35 ppm (two protons on C_4), a multiplet at 1.85 ppm (four equatorial protons on C_3–C_5), a multiplet at 1.7 ppm (four axial

Table I
Properties of PD*n* Polymers

polymer	η, dL/g	χ,[a] %	T_{c1}, °C	T_{c2}, °C	T_1, °C	T_2, °C
PD6	1.40	52			183[b]	310[b]
PD7	0.96	50	252	180	185	269
PD8	1.33	57	253	193	213	271
PD8[c]	2.70	62	260	199	219	280
PD9[c]	3.25	61	231	139	176	254
PD10	2.00	58	230	206	218	248
PD11	0.52	58	213	125	160	230
PD12	1.40	52	208	200	204	225

[a] Percentage of crystallinity. [b] The temperatures were measured in the first run. [c] The polymerization was carried out in a 30% more concentrated solution.

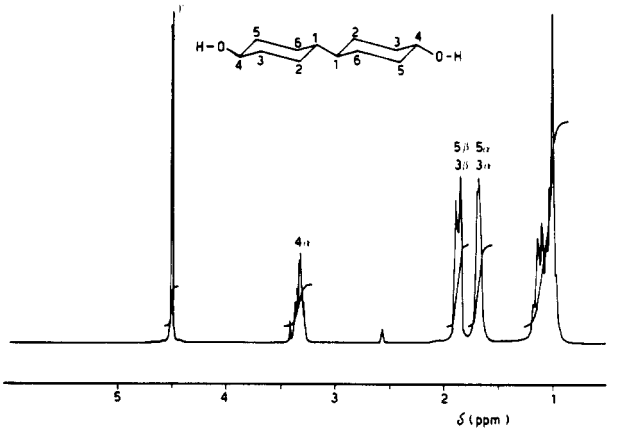

Figure 1. ^{1}H NMR spectrum of dihydroxybicyclohexyl; α = axial H, β = equatorial H, τ = equatorial (-O-)H.

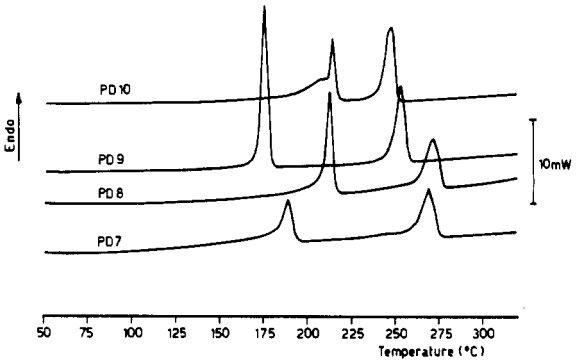

Figure 2. DSC thermograms for PD7–PD10 polymers: heating (second run). Rate: 20 °C/min.

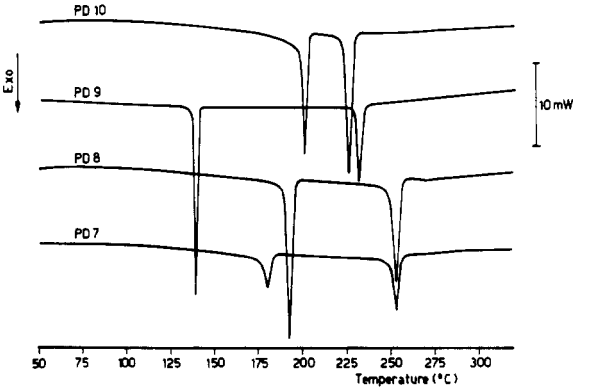

Figure 3. DSC thermograms for PD7–PD10 polymers: cooling. Rate: 10 °C/min.

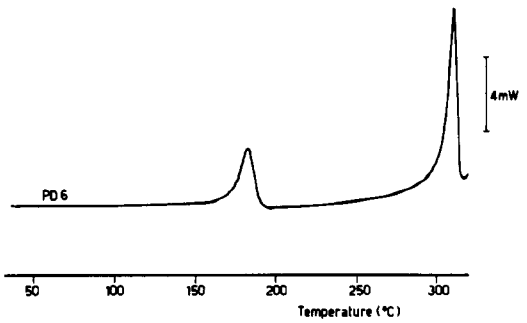

Figure 4. DSC thermogram for the PD6 polymer: heating (first run). Rate: 20 °C/min.

protons on C_3–C_5), and a multiplet at 1.1 ppm (10 protons on C_1–C_2–C_6). The doublet at 4.5 ppm disappeared after treatment with perdeuteroacetic acid (D^4) and was transformed into a singlet by irradiating at 3.35 ppm.

Preparation of Polymers.[4] A total of 2.46 g of *trans,trans*-4,4'-dihydroxybicyclohexane (12.42 mM), an equimolar amount of distilled aliphatic dicarboxylic acid chloride, and 60 mL of 1,2,4-trichlorobenzene were placed under nitrogen in a 100-mL round-bottomed flask, equipped with a mechanical stirrer, condenser, and nitrogen inlet tube. The reaction mixture was refluxed at 220 °C for 3 h, until no more hydrochloric acid was evolved. After cooling to 50 °C, the polymer was precipitated by adding acetone, filtered, and washed with acetone, hot water, and finally an acetone/methanol mixture. After drying under vacuum at 160 °C, the polymers were isolated in almost quantitative yields. They were characterized by thermal analysis (DSC, TGA), optical microscopy, X-ray diffraction, and inherent viscosity.

The main properties of the polymers synthesized are reported in Table I. They are referred to in the present paper as PD*n*, *n* being the number of the methylene groups of the aliphatic dicarboxylic acid.

(III) Results and Discussion

Thermal Analysis. For all synthesized polymers no thermal decomposition below 310 °C was observed by thermogravimetric analysis, carried out according to the conditions described above.

The DSC heating (second run) and cooling curves for PD7–PD10 polymers are reported in Figures 2 and 3, respectively. Cooling and heating curves exhibit two peaks. The low-temperature endotherm (T_1) was interpreted as the crystal melting transition, and the one at higher temperature (T_2), as the isotropization temperature. The reversibility of the phase transitions is evidenced by the presence of two corresponding peaks at T_{c1} (high temperature) and T_{c2} (low temperature) in the cooling curve. Such an interpretation was corroborated by optical microscopy. T_1 is the temperature at which the crystalline solid was transformed to a highly viscous birefringent liquid, and T_2 is the temperature at which the system became isotropic.

The heating (first run) DSC curve for PD6 is reported in Figure 4. For the case of PD6 the isotropization temperature occurs at a temperature coinciding with the onset of the decomposition as observed by TGA and optical microscopy, thus precluding further study.

The heating and cooling DSC curves for PD11 and PD12 polymers are reported in Figure 5. Unlike the other samples, the curves for these polymers indicate a more complex multiple-transition profile from the crystalline to the isotropic phase; i.e., the peaks associated with the two main transitions show evidence of splitting into doublets. This is especially pronounced in the melting endotherms in the heating curves of both samples but also in the crystallization exotherms, i.e., the cooling curve of polymer PD12. No changes can be observed in the polarized microscope as the temperature interval of the doublet is scanned. Further investigations are, therefore, necessary to characterize this behavior. Only the temperature of the main transition is reported in Table I. In this table the properties of PD7–PD11 are summarized. In addition to T_1, T_2, T_{c1}, and T_{c2}, the inherent viscosities and the percentages of crystallinity as determined by X-ray measurements are also reported (see the Experimental Section).

The melting temperatures (T_1) decrease in a regular way with increasing *n* for *n* odd. This effect is due to the decreasing rigidity of the repeating unit of the polymers. For *n* even, however, the melting temperature shows curiously almost no dependence on spacer length. Moreover, an odd–even effect was detected in the variation of the crystalline melting transition with the length of the spacer as shown in Figure 6, as expected for polymers containing flexible spacers.[6] Also the clearing temperatures decrease by enhancing the number of methylene units, but in this case the odd–even effect was not so evident: an approximately linear dependence was observed. The consequence is that the range of mesophasic stability is greater for those polymers with odd numbers of methylene units in the spacers. Analogous examples have already been reported in the literature.[10-12]

In Table II the most important transition parameters are summarized. ΔH and ΔS are the experimental enthalpy and entropy per mole of repeating unit associated with the respective transitions. Neither a regular variation of ΔS_2 (the isotropization entropy) nor the odd–even effect was observed with the variation of the spacer length.[6d,13]

The elevated values of ΔH_2 and ΔS_2 are typical of a transition from a highly ordered smectic phase to the isotropic phase. Similar values have been reported for the S_H–I transition in the corresponding even-membered aromatic series.[8] However, on comparison of the two classes of polymers, two main differences can be pointed out:

(1) In the spacer length range of 7–10 methylene units, only one mesomorphic phase was observed for the polymers reported here independent of spacer length. On the contrary, in the corresponding aromatic polymers the mesophase is smectic for the even-membered examples, while smectic–nematic polymorphism can be detected in the odd-membered ones, at least for low molecular weights.[7,8]

(2) The range of mesophase stability for the *odd*-membered polymers is markedly different for the two series. As shown in Table II, the range is 80–100 °C for PD*n* while less than 30 °C was reported for the biphenyl derivatives. This behavior shows that the thermodynamic stability of the mesophase is affected by geometric repulsive factors more than the polarizability of the mesogenic group.

The dominance of geometric factors relative to polarizability effects was postulated long ago by Vörlander.[1m] Since that time, the question has been the subject of continuing debate regarding the relative merits of the Flory–Onsager approach, relating to repulsive geometric factors on the one hand, and the Maier–Saupe approach, relating to polarizability attractive factors on the other. This discussion has been the subject of a review.[14] Literature data for low molecular weight compounds show not only that formation of highly ordered smectic phases in disubstituted *trans,trans*-4,4'-bicyclohexanes[2] is possible but also that the ranges of stability of the mesophases are larger than those in the corresponding diphenyl compounds. Our experimental data can thus be inter-

Table II
Calorimetric Transition Parameters for PD*n* Polymers

polymer	T_1, K	ΔH_1,[a] kcal/mol	ΔS_1,[a] eu	T_2, K	ΔH_2, kcal/mol	ΔS_2, eu	$\Delta S'_{total}$,[b] eu	ΔS_1*,[c] eu	ΔS_2*,[d] eu	ΔS^*_{total},[e] eu
PD7	458	3.90	8.52	542	4.03	7.44	8.72	4.77	2.08	6.85
PD8	486	4.30	8.85	544	3.72	6.84	10.90	4.54	2.10	6.64
PD9	449	5.75	12.81	527	3.98	7.56	13.08	7.00	2.52	9.52
PD10	491	5.82	11.86	521	4.28	8.21	15.26	7.30	2.93	10.23

[a] Apparent enthalpy and entropy variations, uncorrected for degree of crystallinity. [b] $\Delta S'_{total} = k \ln 3^{n-3}$. [c] $\Delta S_1^* = (\Delta S_1/\chi) W(CH_2)/W_{total}$. [d] $\Delta S_2^* = \Delta S_2 W(CH_2)/W_{total}$. [e] $\Delta S^*_{total} = \Delta S_1^* + \Delta S_2^*$.

Table III
Optical Transition Temperatures of PD*n* Polymers[a]

polymer	T_a, °C	T_b, °C	T_c, °C
PD7	181	267	254
PD8	220	268	249
PD9	175	249	227
PD10	218	252	215

[a] T_a = melting point (heating rate 10 °C/min). T_b = clearing temperature (heating rate 10 °C/min). T_c = isotropic–birefringent liquid transition (cooling rate 10 °C/min).

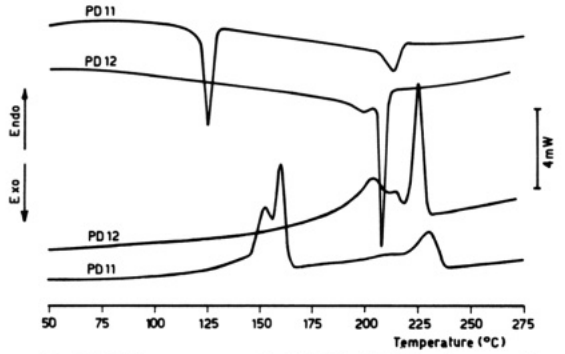

Figure 5. DSC thermograms for PD11–PD12 polymers: heating (second run) and cooling. Rate: as previously.

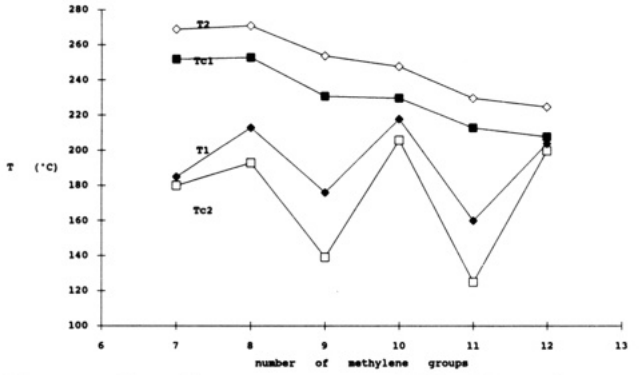

Figure 6. Transition temperatures of PD7–PD12 polymers: T_1, crystal–mesophase; T_2, mesophase–isotropic liquid; T_{c1}, isotropic liquid–mesophase; T_{c2}, mesophase–crystal.

preted as follows: the packing of the flat phenyl group is not as effective as that of a cyclohexyl. By replacement of both phenyls by cyclohexyl moieties, a higher degree of packing efficency and hence a thermodynamically more stable mesophase are obtained, even if the mesogenic aspect ratio (length/diameter) remains practically the same (2.26 for biphenyl and 2.27 for bicyclohexyl). Since the stability of the mesophase is influenced by molecular interactions, related to the intermolecular separation, and *odd* number of methylene units in the spacer seems to imply a conformation that hinders a dense packing in the aromatic series. On the contrary, an *even* number of methylene units seems to allow a dense packing of the mesogenic groups in both series of polymers with the consequence of equal mesogenic stability.

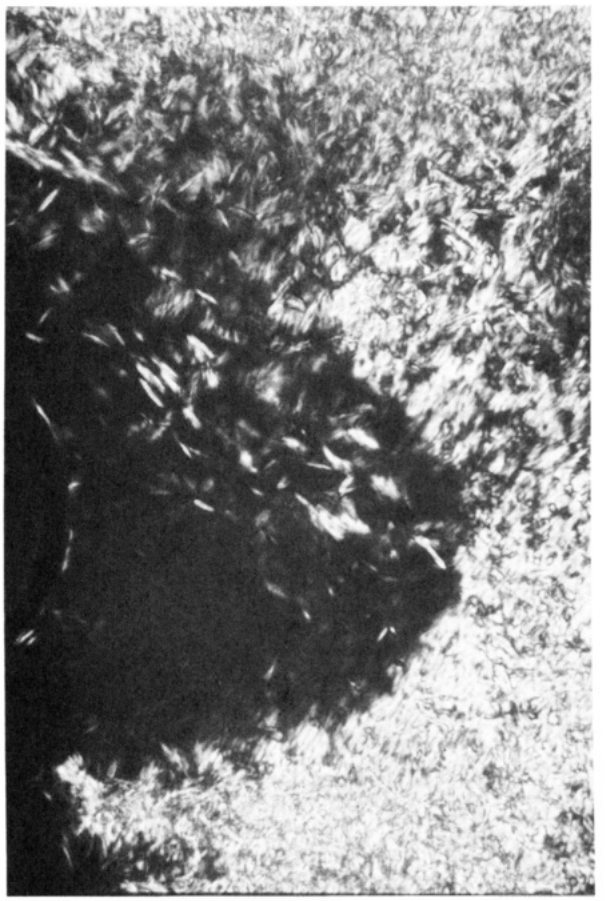

Figure 7. Optical micrograph showing the mesophasic texture of the PD8 polymer at 263 °C on cooling from isotropic melt at 2 °C/min. Cross polars; magnification 1050×. (The original has been reduced 40%.)

One can observe in Table II that ΔH_1 increases with spacer length while ΔH_2 appears to be independent. ΔS_1 and ΔS_2 show no obvious trends. The fact that the sum of ΔS_1 and ΔS_2 is the entropy of the crystal–isotropic liquid transition associated with the conformational variation of the aliphatic fragment of the repeating unit enables one to calculate the total entropy involved in the series of transitions. Approximating this case to that of an isolated aliphatic chain, one can use the formula $\Delta S' = k \ln 3^{n-3}$ for a tetrahedral chain that undergoes the transition from the crystal in an all-trans conformation, i.e., a single configuration to an amorphous liquid with a freely rotating chain, i.e., 3^{n-3} configurations. In this formula k is the gas constant and n the number of carbon atoms in the chain. The results for n ranging from 7 to 10 are summarized in Table II. Also reported in Table II are the experimentally found values of the entropy, appropriately corrected for the crystalline content and the relative fraction of the aliphatic chain in the repeat unit, $W(CH_2)/W_{total}$, $W(CH_2)$ being the weight of the aliphatic fragment in a repeat unit of weight W_{total}. These corrected values are referred to as ΔS_1^* and ΔS_2^* (see footnotes *c* and *d* of Table II). The calculated values of the total entropy $\Delta S'$ parallel those

Figure 8. Optical micrograph of the mesophasic texture for the PD10 polymer at 233 °C on cooling from isotropic melt with a rate of 20 °C/min. Crossed polars; magnification 1050×. (The original has been reduced 40%.)

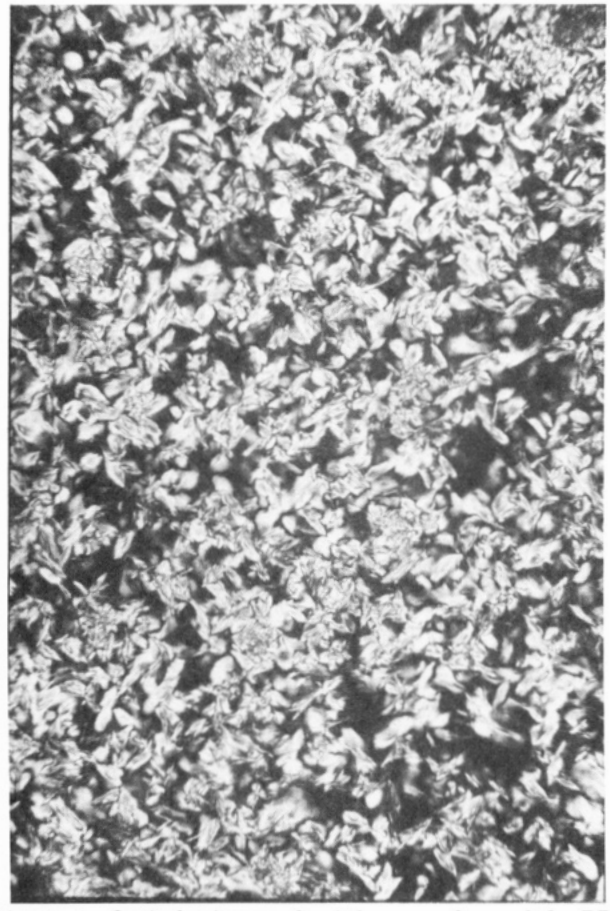

Figure 9. Optical micrograph of the mesophase of the PD9 polymer at 189 °C after 30 min of annealing. Crossed polars; magnification 430×. (The original has been reduced 40%.)

experimentally found for ΔS_{total}*; i.e., a marked increase is shown with spacer length from samples PD7/PD8 to PD9/PD10. This would be consistent with the overall increase in entropy from the crystalline to isotropic state if the aliphatic chains were in the fully extended conformation in the crystal and reverted to a completely random conformation in the isotropic liquid.

Optical Microscopy. The transition temperatures of PD7–PD10 obtained by optical microscopy are reported in Table III. These are in good agreement with those recorded by DSC. Melting at T_a led in all examined cases to the formation of a very viscous and slightly birefringent phase, which does not allow a clear identification of characteristic textures. Similar behavior was also observed in the case of the corresponding highly ordered phases for the aromatic polyesters. Upon cooling from the isotropic liquid, a birefringent phase forms at T_c as spherical-shaped particles, which, upon further cooling, assume oblong shapes (bâtonnets), ultimately developing a fanlike texture. The fans are in all cases small, as can be expected from polymers having a high molecular weight and melt viscosity. Figures 7–9 show typical textures of PD*n* in the mesophase obtained by cooling the isotropic liquid. Figure 7 shows the texture of PD8 at 263 °C upon cooling (cooling rate: 2 °C/min). Bâtonnets can be noted in the center of the photo, while a fully developed mesophase is present at the edges (magnification 1050×). In Figure 8 is reported a typical fanlike texture of the PD10 polymer at 233 °C upon cooling at a rate of 20 °C/min (magnification 1050×). Well-developed fans are shown in Figure 9 for the polymer PD9 annealed at 189 °C after cooling from the isotropic melt (magnification 430×).

The transition from isotropic liquid to the mesophase appears to be faster in the case of even-membered PD*n* than odd ones. The kinetics of this transition are at present under investigation in order to clarify the influence of structure on transition rate. No comment can be made regarding the crystallization transition because of the difficulty in detecting it by optical microscopy.

X-ray Diffraction Analysis. In order to clarify the structure of PD*n*, particularly in the mesophase, X-ray diffractometric measurements were performed on PD8 and PD9 as models for even and odd representatives of the series, respectively. For every sample four X-ray pictures were recorded: (1) at room temperature, (2) above the crystalline–mesophase transition, (3) in the mesophase after cooling from isotropic melt, and (4) at room temperature after a complete heating and cooling cycle. In all cases (1) was the same as (4) and (2) was the same as (3). Figures 10a and 11a are the diffraction patterns, respectively, of the crystalline phases of PD8 and PD9, and Figures 10b and 11b are those of the mesophases of PD8 and PD9 polymers, respectively.

In Figure 10b, the mesophase of PD8, it is possible to observe an inner ring of very weak intensity and two outer rings, corresponding, respectively, to 15.67, 4.75, and 2.74 Å. In particular, the intensity of the first outer ring at 4.75 Å is very strong. In Figure 11b, the mesophase of PD9, the same diffraction pattern was observed: an inner ring of low intensity corresponding to 16.1 Å, an outer ring of strong intensity to 4.81 Å, and a second outer ring to 2.76 Å.

For both polymers the ratio of interplanar spacing corresponding to the two outer rings is about $\sqrt{3}$. It suggests a regular hexagonal packing in a plane perpendicular to

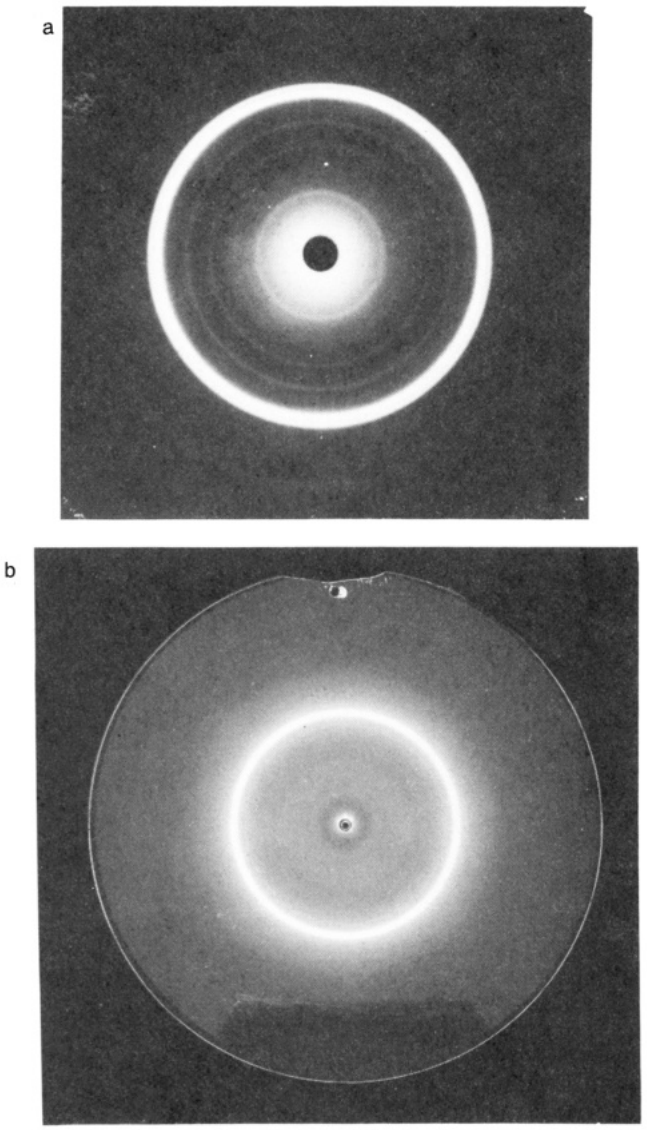

Figure 10. Diffraction patterns for the PD8 polymer: (a) crystalline phase at 30 °C, (b) smectic phase at 210 °C. (The originals have been reduced 60%.)

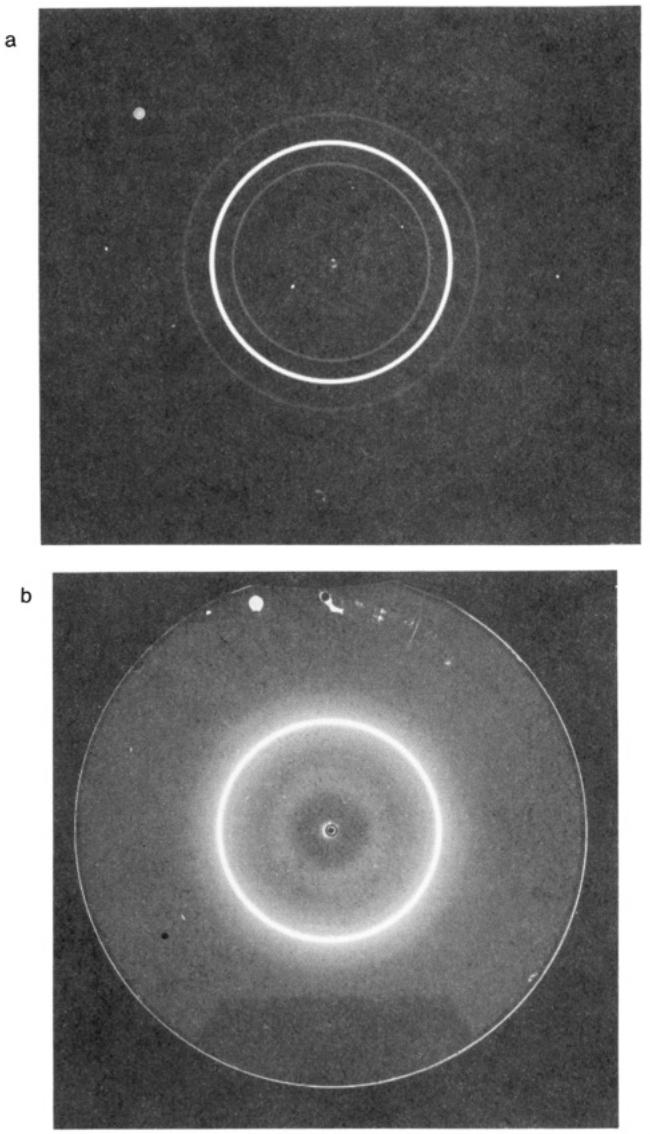

Figure 11. Diffraction patterns for the PD9 polymer: (a) crystalline phase at 30 °C, (b) smectic phase at 200 °C. (The originals have been reduced 60%.)

the long molecular axis, and from the positions of all Bragg peaks a monoclinic unit cell was derived. The lattice parameters, refined by using a computer program that minimizes the difference between the experimental and calculated data, are reported in Table IV. The experimental $D(hkl)$ values, the relative intensities, and the calculated $D(hkl)$ values are also summarized in this table. The good agreement found between the calculated and experimental data supports the validity of the lattice parameters obtained.

The overlap of (110) and (200) peaks can explain the high experimental intensity found for both polymers in the mesophase. The $\sqrt{3}$ is the ratio of the spacing corresponding to (110) and (020) peaks. In conclusion, both PD8 and PD9 polymers in the mesophase are arranged within layers containing perfect hexagonally close-packed arrays of molecules with their long axes tilted with respect to the layer planes (see Figure 12). This arrangement corresponds to a smectic G phase. The tilt angles ($180 - \beta$) for PD8 and PD9 are very similar ($\beta = 52.5°$ for PD8 and $\beta = 51.4°$ for PD9). The molecular axes seem more tilted relative to the values reported in the literature[15] for low molecular weight liquid crystals.

Many rings appear in the diffraction pattern of the crystalline phases; i.e., Figures 10a and 11a. Their positions and intensities are reported in Table IV. The lattice parameters for the crystalline phase obtained by using the same procedure as that for the mesophase are also shown in the same table. The sharp inner ring (corresponding to 14.74 Å for PD8 and 15.84 Å for PD9) was indexed as the (001) reflection. The intensity of the first outer ring, 4.49 Å for PD8 and 4.45 Å for PD9, is very strong and was indexed as the (110) peak. The crystalline phases of both compounds also are monoclinic unit cells; i.e., the molecules have pseudohexagonal close packing but are characterized by cell parameters different from those of the mesophase.

Calculated Estimate of the Repeating Unit 3-Dimensional Structure Based on Conformational Analysis. To obtain information on the preferred conformations of PD8 and PD9 repeating units, in the crystalline and smectic phases, the molecular mechanics method CSD (conformations statistical distribution) was utilized. The theoretical basis of this methodology has been reported elsewhere.[16] Through this type of calculation the following results can be obtained for any isolated molecule: (1) probability of every calculated conformation; (2) statistical weight of the possible conformational minima; (3) 3D structure of the molecule in every minimum (cluster) as a result of the weighed average of the

Table IV
Experimental and Calculated Bragg Spacings for PD*n* Polymers

Polyester with 8 Methylene Groups

crystalline phase[a]				smectic phase[b]			
exptl data		calcd data		exptl data		calcd data	
D(*hkl*)	intens	*D*(*hkl*)	*hkl*	*D*(*hkl*)	intens	*D*(*hkl*)	*hkl*
14.72	1	14.70	001	15.67	2	15.67	001
11.12	7	11.09	101	6.56	2	6.57	103
8.41	2	8.42	100	5.25	7	5.22	003
6.47	15	6.46	103	4.75	100	4.75	110/200
5.89	19	5.84	$10\bar{1}$	3.93	1	3.92	004/211
4.97	1	4.96	011	2.74	2	2.74	020
4.49	100	4.47	110				
4.32	60	4.31	$10\bar{2}$				
3.84	4	3.82	212				
3.30	20	3.29	210				
3.01	1	3.02	014				

Polyester with 9 Methylene Groups

crystalline phase[c]				smectic phase[d]			
exptl data		calcd data		exptl data		calcd data	
D(*hkl*)	intens	*D*(*hkl*)	*hkl*	*D*(*hkl*)	intens	*D*(*hkl*)	*hkl*
15.84	12	15.82	001	16.10	1	16.10	001
12.02	1	12.01	101	6.82	2	6.84	103
8.56	2	8.56	100	5.83	1	5.81	203
7.90	4	7.91	002	5.32	3	5.36	003
5.93	2	5.94	$10\bar{1}$	4.81	100	4.81	110/200
5.35	25	5.37	104	3.98	2	3.97	211
4.92	1	4.94	$00\bar{1}$	2.76	2	2.78	020
4.45	100	4.45	110	4.27	1	4.28	200
4.27	1	4.28	200	3.94	2	3.96	004
4.08	1	4.08	105				
3.94	2	3.96	004				
3.81	1	3.79	214				
3.70	18	3.71	013				
3.54	6	3.54	$20\bar{1}$				
3.32	2	3.31	210				
3.09	2	3.10	405				
2.93	2	2.93	$21\bar{1}$				
2.63	2	2.61	020				
2.55	2	2.57	021				

[a] T = 30 °C. Derived unit cell parameters: a = 11.16 Å; b = 5.27 Å; c = 19.48 Å; β = 49.0°. [b] T = 220 °C. Derived unit cell parameters: a = 11.98 Å; b = 5.48 Å; c = 19.76 Å; β = 52.5°. [c] T = 30 °C. Derived unit cell parameters: a = 12.4 Å; b = 5.21 Å; c = 23.0 Å; β = 43.5°. [d] T = 210 °C. Derived unit cell parameters: a = 12.3 Å; b = 5.55 Å; c = 20.6 Å; β = 51.4°.

Table V
Calculated Conformational Features of PD*n* Polymers

		cluster 1			cluster 2		
polymer	T, °C	probability, %	$l_{BA'}$,[a] Å	$l_{A'B'}$,[a] Å	probability, %	$l_{BA'}$,[a] Å	$l_{A'B'}$,[a] Å
PD8	60	42	7.48	21.97	18	17.81	18.91
PD8	225	41	7.48	21.92	24	18.42	18.92
PD9	60	60	19.42	18.81	30	21.40	18.60
PD9	210	58	18.06	18.80	36	17.40	18.60

[a] l = length of the noted sequence.

Table VI
Comparison between Calculated Values of Some Steric Parameters for PD*n* Polymers As Obtained by X-ray Diffraction and Conformational Analysis

		values calcd from X-ray diffractn data			values calcd from conformatnl anal.		
polymer	T, °C	d,[a] Å	c, Å	β, deg	d,[a] Å	c, Å	β, deg
PD8	30	14.72	19.5	49	14.9	18.9	52
PD8	225	15.67	19.8	52.5	16.0	18.9	58
PD9	30	15.84	23.0	49.5	15.0	21.4	44
PD9	210	16.10	20.6	51.4	14.0	17.4	52

[a] d is the azimuthal layer line spacing for the crystal lattice or the smectic phase.

conformations belonging to the cluster.

The latter is the most important because it is a good simulation of X-ray results. In this way experimental and theoretical values of structural parameters, such as smectic layer spacings and molecular chain extensions, can be compared. One can observe if the two sets of data are mutually consistent and support the same hypothesis of crystalline packing.

Since CSD can deal with only one single molecule at a time, we have to formulate a microscopic model simulating

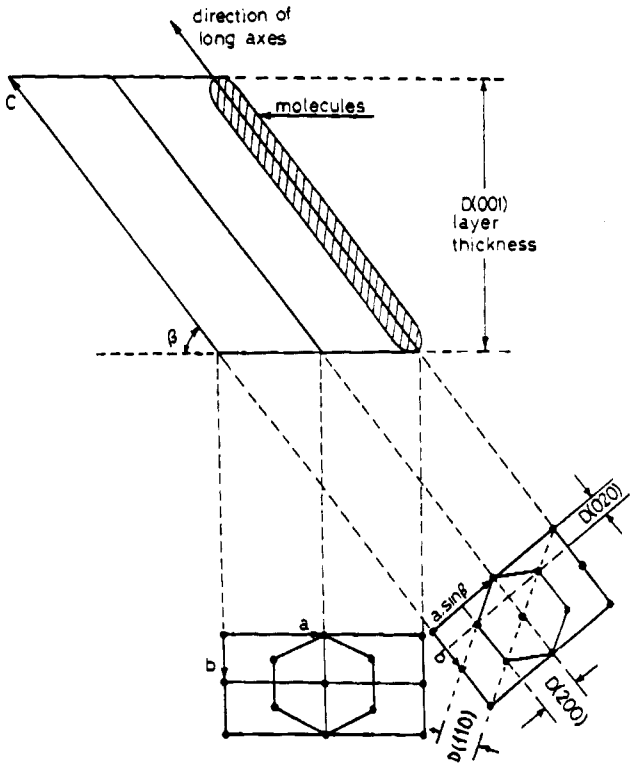

Figure 12. Disposition of the PD8 and PD9 molecules in the smectic unit cell.

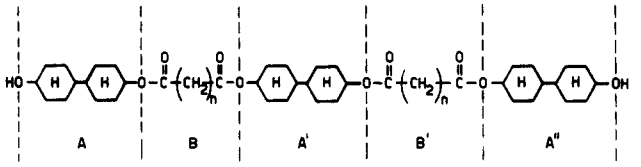

Figure 13. Oligomeric fragment of PD*n* subject to conformational analysis.

conformational constraints induced by neighboring molecules for a chain in the bulk. Moreover, such a model has to simulate the polymeric chain extension even if only a limited number of atoms can be dealt with. For both polymers we have chosen the simplified model formed by two and a half repeating units as shown in Figure 13. In this modeling approach the most meaningful segments representing chain repeat units are BA′ and A′B′. Their positions inside the chain fragment do not allow the rotational freedom that the repeat unit would have if it were isolated. The existence of two equivalent representative segments is due to the presence of the A″ moiety. It was added in order to limit the rotational freedom of aliphatic moiety B′. However, B and B′ are only topologically equivalent, since generally they show different average conformations in the statistical calculation, leading to more detailed information about the 3D structure.

Finally, rotations around single bonds were not performed simultaneously. Only small groups of adjacent bonds were moved consecutively, simulating as near as possible the conformational freedom in the bulk. One can in fact assume that in the bulk only local movements are important, since long-range intramolecular interactions would be dominated by the intermolecular ones.

A preliminary calculation of all acceptable[17] conformations was performed for both PD8 and PD9 chain models, and the most probable clusters were determined. The results obtained in the range of stability of the crystalline and smectic phases are summarized in Table V.

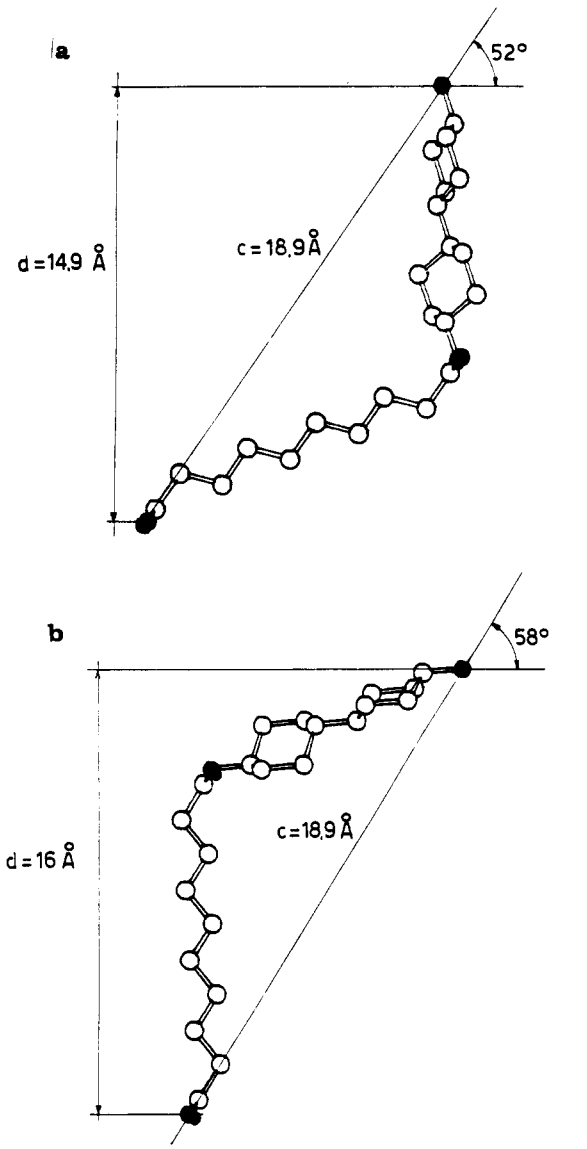

Figure 14. Most probable conformation of the polymer PD8 in (a) the crystalline phase at 30 °C and (b) the mesophase at 210 °C.

The conformations derived from cluster 2 in both cases seem to agree most satisfactorily with the experimental results. In particular, in these clusters, the molecular fragments assume more extended conformations, as would be expected for the bulk crystalline state. We have assumed the repeating unit length, *l* or *l*′, to be coincident with the parameter *c* in the experimental unit cell. Thus for PD8, the A′B′ segment was taken as the representative repeat unit, because its length does not vary with temperature. On the contrary for PD9, the segment BA′ represents the repeat unit because it shows the largest variation with temperature, as indicated from parameter *c* values in the unit cell, e.g., in Table IV.

These results were the starting point for another more detailed conformational analysis. To better simulate the constraints due to chain extension at the ends of the repeat unit, only bonds inside the repeat units were allowed to rotate. The remainder of the molecular fragments were kept fixed. The refined results so obtained indicate that both polymers have extended configurations belonging to a cluster of a very high probability (>80%). However, no substantial differences were observed for A′B′ and BA′ sequence lengths as previously reported for cluster 2 in Table V.

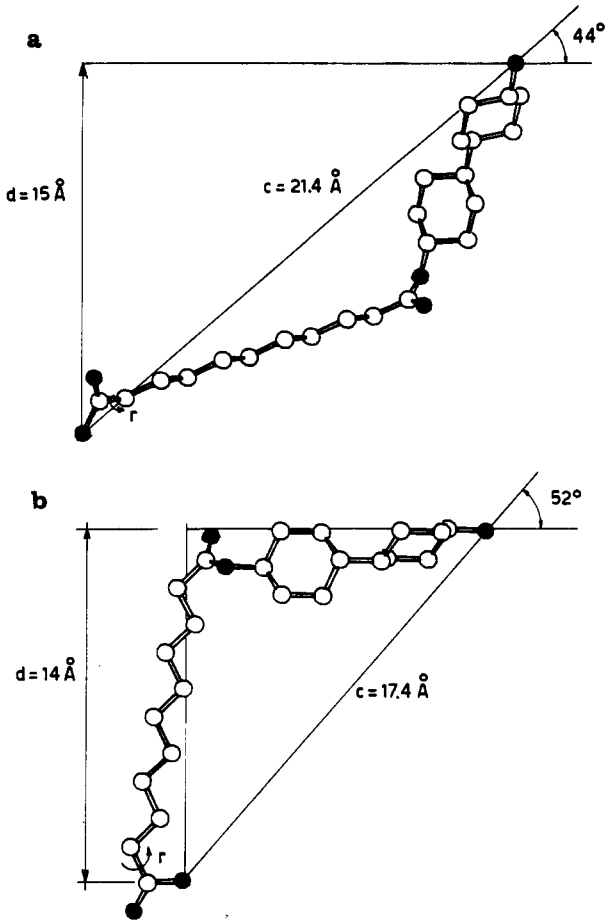

Figure 15. Most probable conformation of the PD9 polymer in (a) the crystalline phase at 30 °C and (b) the mesophase at 200 °C.

The obtained preferred conformations indicate that the main difference between these two polymers in the crystalline phase is in the relative steric disposition of A and B type moieties. For PD8 a trans disposition of bicyclohexyl groups, A, relative to the aliphatic chain B between them is clearly preferred. On the contrary, for PD9, gauche and cis dispositions are energetically preferred. In every case the aliphatic chain B has the all-trans, extended conformation.

By increasing the temperature to the stable limit of the mesophase, only small conformational variations were observed in the case of the PD8 repeat unit. This means that the solid-phase-ordered packing is largely maintained in the mesophase. This is not the case with the PD9 repeat unit because a greater variation of steric features was observed in the temperature range covering the crystalline to smectic phase transition.

Positions of repeat units between ordered planes in the crystalline and smectic phases of PD8 and PD9 (β angles) consistent with measurements and calculations are indicated in Figures 14 and 15. This hypothesis is very similar to the one already proposed for the case of polymers derived from dihydroxydiphenyl. Table VI summarizes and compares values obtained from X-ray and conformational analysis for some selected steric parameters of PD8 and PD9 polymers. Good agreement exists between the two sets of values in particular with respect to trends. The lesser agreement observed in the case of parameters d and c of PD9 in the smectic phase is not surprising, however, taking into account (1) the large experimantal error associated with the diffuse and very weak inner diffraction rings and (2) the large rotational freedom around the bond connecting the aliphatic chain B to the mesogenic moiety A' (see "r" in Figure 15), giving rise to conformations of very similar energy but with different c and d values.

According to the hypothesis presented here, one can conclude that it is very likely that during a crystal–smectic transition only a mutual sliding of polymeric chains occurs for PD8. For PD9 this phenomenon has to be accompanied also by significant conformational changes, such as the ones described above.

(IV) Conclusion

Thermotropic liquid-crystalline polyesters have been prepared on the basis of the 4,4'-dihydroxybicyclohexyl mesogenic unit and linear aliphatic diacids. They have been shown to exhibit a smectic G phase. The spacer has been found to be in an extended chain conformation. Both crystalline and isotropic phases are also found to be present. The polymers follow the usual pattern displayed by mesogenic core–flexible spacer polymers.

References and Notes

(1) (a) Braun, D.; Hirschmann, H.; Herrmann-Shönherr, O.; Lienert, M.; Wendorff, J. H. *Makromol. Chem., Rapid Commun.* **1988**, *9*, 309. (b) Clausen, K.; Kops, J.; Rasmussen, K.; Rasmussen, K. H.; Sonne, J. *Macromolecules* **1987**, *20*, 2660. (c) Osman, M. A. *Polymer* **1987**, *28*, 713. (d) Braun, D.; Schulke, U. *Makromol. Chem.* **1986**, *187*, 1145. (e) Osman, M. A. *Makromol. Chem., Rapid Commun.* **1986**, *7*, 183. (f) Osman, M. A. *Macromolecules* **1986**, *19*, 1824. (g) Kwolek, S. L.; Luise, R. R. *Macromolecules* **1986**, *19*, 1786. (h) Polk, M. P.; Bota, K. B.; Nandu, M.; Phingbodhipakkiya, M.; Edeogu, C. *Macromolecules* **1984**, *17*, 129. (i) Kyotani, M.; Kanetsuna, H. *J. Polym. Sci., Polym. Phys. Ed.* **1983**, *21*, 379. (j) Polk, M. P.; Bota, K. B.; Akubuiro, E. C.; Phingbodhipakkiya, M. *Macromolecules* **1981**, *14*, 1626. (k) Jackson, W. J., Jr.; Darnell, W. R. U.S. Patent 4,342,862, 1981. (l) Schaefgen J. R. U.S. Patent 4,118,372, 1981. (m) Vörlander, D. *Z. Phys. Chem.* **1923**, *105*, 211.

(2) (a) Eidenschink, R.; Erdmann, O.; Krause, J.; Pohl, L. *Angew. Chem., Int. Ed. Engl.* **1978**, *17*, 133. (b) Brownsey, G. J.; Leadbetter, A. J. *J. Phys. Lett. (Paris)* **1981**, *42*, L.135. (c) Osman, M. A. *Z. Naturforsch.* **1983**, *38A*, 639. (d) Mallon, J. J.; Kantor, S. W. *Macromolecules* **1989**, *22*, 2070.

(3) Ringsdorf, H.; Schneller, A. *Br. Polym. J.* **1981**, *13*, 43 and references therein.

(4) Coassolo, A.; Gardano, A.; Foá, M.; Chapoy, L. L. European Patent Application 300,751, 1987.

(5) Gardano, A.; Casagrande, F.; Foá, M.; Petrini, G.; Barisone, R.; Chapoy, L. L. European Patent Application 290,239, 1987.

(6) (a) Roviello, A.; Sirigu, A. *J. Polym. Sci., Polym. Chem. Ed.* **1975**, *13*, 455. (b) de Gennes, P.-G. *C. R. Acad. Sci. (Paris) Ser. B* **1975**, *281*, 101. (c) Krigbaum, W. R.; Ciferri, A.; Asrar, J.; Toriumi, H.; Preston, J. *Mol. Cryst. Liq. Cryst.* **1981**, *76*, 99. (d) Ober, C. K.; Jin, J. I.; Lenz, R. W. *Advances in Polymer Science*; Springer-Verlag: Berlin, 1984; Vol. 59, pp 104–146.

(7) Asrar, J.; Toriumi, H.; Watanabe, J.; Krigbaum, W. R.; Ciferri, A. *J. Polym. Sci., Polym. Phys. Ed.* **1983**, *21*, 1119.

(8) Krigbaum, W. R.; Watanabe, J.; Ishikawa, T. *Macromolecules* **1983**, *16*, 1271.

(9) (a) Wilds, A. L.; Shunk, C. H.; Hoffman, C. H. *J. Am. Chem. Soc.* **1954**, *76*, 1733. (b) Wilds, A. L.; Pearson, T. H.; Hoffman, C. H. *J. Am. Chem. Soc.* **1954**, *76*, 1737.

(10) Jin, J. I.; Antoun, S.; Ober, C. K.; Lenz, R. W. *Br. Polym. J.* **1980**, *12*, 132.

(11) Ober, C. K.; Jin, J. I.; Lenz, R. W. *Makromol. Chem., Rapid Commun.* **1983**, *4*, 49.

(12) Kricheldorf, H. R.; Pakull, R. *Macromolecules* **1988**, *21*, 551.

(13) Luckhurst, G. R. In *Recent Advances in Liquid Crystalline Polymers*; Chapoy, L. L., Eds.; Elsevier Science Publishing Co.: New York, 1986; pp 105–127.

(14) Toriumi, H.; Samulski, E. T. *Mol. Cryst. Liq. Cryst.* **1983**, *101*, 163.

(15) Doucet, J.; Levelut, A. M. *J. Phys.* **1977**, *38*, 1163.

(16) Scordamaglia, R.; Barino, L. In *QSAR and Strategies in the Design of Bioactive Compounds*; Seydel, J. K., Ed.; VCK: Weinheim, 1985; p 299.

(17) Barino, L.; Scordamaglia, R. In *Integration of Fundamental Polymer Science and Technology*; Lemstra, P. J., Kleintjens, L. A., Eds.; Elsevier Applied Science: London, 1980; p 126.